

**IN-VITRO PET IMAGING OF A MINIATURE VENTRICULAR ASSIST DEVICE**

Michael S. Gossman<sup>1,2</sup>, Joel D. Graham<sup>3</sup>, Stephen Depot<sup>3</sup>, Huaiyu Zheng<sup>4</sup>, Junling Li<sup>4</sup>,

Chin K. Ng<sup>4</sup>, Daniel Tamez<sup>3</sup>

<sup>1</sup> Regulation Directive Medical Physics, 104 Hildee Court, Russell, KY 41169, (606) 232-9283, [msgossman@hotmail.com](mailto:msgossman@hotmail.com), <sup>2</sup> Exponent, Inc., Biomedical Engineering Division, Philadelphia, PA, <sup>3</sup> HeartWare, Inc., Miami Lakes, FL, <sup>4</sup> University of Louisville School of Medicine, Department of Radiology, Louisville, KY.

## **ABSTRACT**

Interactions between the life-sustaining ventricular assist devices (VAD) and diagnostic therapies must be carefully considered to decrease the risk of inaccurate diagnostic imaging or pump failure. The HeartWare MVAD pump, currently under investigational use, was tested for interaction with radioactive tracers in an in-vitro loop study. Contrast radiotracers  $^{18}\text{F}$ -sodium fluoride and  $^{18}\text{F}$ -fluorodeoxyglucose were injected into a closed loop to determine feasibility of direct imaging of the MVAD pump in a PET scanner. No real-time changes were observed in pump operation with no statistical difference of pump parameters (power consumption, speed, estimated flow) between baseline and treatment conditions. In addition, no effect on external components including the PAL controller and batteries powering the device was observed. Imaging of the internal pump components was possible with obstruction only observed in the portion of the pump where the rotating impeller is located. Minimal retention of radiotracer in the pump components following circulation was measured (<1%). PET imaging is an attractive diagnostic tool for VAD patients and may have additional utility outside of current use in detection of infection.

Running Title: PET imaging with the HeartWare MVAD pump

Key words: MVAD, PET, pump, radioactive, ventricular assist device

## **INTRODUCTION**

The use of ventricular assist devices (VAD) in severe heart failure patients is increasing due to the extent of wait time for heart donors (1-4). As a result, VADs have been utilized as a means for bridge to transplant and destination therapy, until a heart transplant becomes readily accessible (5-7). The MVAD pump (HeartWare, Inc.; Miami Lakes, FL) is a mechanical assist device with continuous, axial blood flow (currently for investigational use only) (5,8). The miniaturized design allows implantation in smaller sized patients and a potential reduction in length of stay through use of less-invasive surgery such as a thoracotomy approach (9,10). The MVAD pump contains a wearless impeller suspended in a motor core through passive magnetic and hydrodynamic forces rotating at a range of 8,000 to 18,000 rpm. The aim of this study addresses the use of positron emission tomography (PET) on operation of the MVAD pump. Secondary aims were detection of potential scattering and attenuation in the imaging as well as retention levels of gamma radiation in the MVAD pump. Figure 1 portrays the surgical position of the MVAD relative to the anatomy of the heart. The directional flow of pumped blood can be immediately visualized.

Positron Emission Tomography is a non-invasive, nuclear procedure commonly used for detection of cancer and heart disease. The system detects pairs of gamma rays emitted indirectly by a positron-emitting radionuclide introduced into the body on a biologically active molecule. Three-dimensional tomographic images of tracer concentration are constructed by computer analysis. Radionuclides used in PET scans are called contrast agents. These are typically isotopes with short half-lives such as  $^{13}\text{N}$  (10 min) and  $^{18}\text{F}$  (110 min). These contrast agents are incorporated into compounds normally used by the body such as glucose and are known as radiotracers. PET technology traces the biologic pathway of compounds in-vivo providing quantitative parameters of cell viability, proliferation, and metabolic activity of tissue. Two commonly used radiotracers in clinical scanning are fluorodeoxyglucose (FDG) and  $^{18}\text{F}$ -Sodium Fluoride (NaF). FDG is used

primarily for oncology in the majority of scans internationally. NaF is commonly used for detecting and evaluating metastatic bone cancer. (11,12)

In the clinical setting, there is concern of scattering or attenuation during imaging due to the metallic device components. Another concern is the retention of radioactivity in the MVAD pump following injection of radiopharmaceuticals instead of the intended circulation to biological tissue. This could potentially cause artifact with imaging. Consequently, undesirable contrast and resolution can lead to a potential error in diagnosis. Use of PET imaging in the VAD patient population is limited with recent reports for detection of infection (1,13-15). In this study, PET imaging was utilized to examine the imaging capability of the MVAD pump in an in-vitro flow loop with two commonly used radiopharmaceuticals, NaF and FDG.

## **MATERIALS & METHODS**

A MVAD pump with an attached 10mm outflow graft (Vascutek; UK) was connected to a 1.2 L in-vitro flow loop filled with deionized water and glycerin at a 2:1 mixture ratio. The system components included the HeartWare PAL controller, alternating current adaptor, and battery. The controller manages power, monitors pump function, provides diagnostic information, and stores pump parameter data. A laptop with a custom Labview program (National Instruments; Austin, TX) and data acquisition system, PAL-DAS, was used to set controller settings and record real-time pump parameters. A Siemens MicroPET-R4 scanner (Siemens; Knoxville, TN) was used for imaging with a 1.8 mm spatial resolution at the center of the field-of-view. All images were reconstructed using an OSEM2D algorithm and analyzed by ASIPro software with all quality assurance checks and calibrations prior to imaging.

NaF was synthesized in house and FDG was purchased from PETNET Solutions, Inc., Molecular Imaging Research Center (Louisville, KY). Briefly,  $^{18}\text{F}$ -fluoride was diluted with deionized water and passed through a cation exchange ( $\text{H}^+$  form) cartridge and a Sep-Pak Accell Plus QMA cartridge. The cation cartridge was removed and the QMA cartridge was rinsed with 10 mL sterile water and air dried. The FDG radiotracer was received as used clinically and required no cation exchange. Both radiotracers were diluted with 5-10 mL of saline and passed through a 0.2  $\mu\text{m}$  filter to provide the end product for imaging. The typical injected activity for PET contrast is 15 milliCuries (mCi). Assuming normal total blood volume of 5 L for an adult, the concentration needed for the 1.2 L in-vitro flow loop was calculated to be 3.6 mCi.

The flow loop was placed in the scanner with the MVAD pump placed in the center of the imaging bore as seen in Figure 2. The loop reservoir was placed adjacent to the scanner and surrounded with lead bricks to significantly reduce the contribution of the external source to the final imaging counts. The pump was connected to the permissive action link controller and started. The speed was increased to 14,000 RPM (within recommended speed operation range) providing a controller estimated flow of 6.2 L/min. After a 5 minute circulation time with no radiopharmaceutical present, the PET scanner acquired a baseline image set over 10 minutes. The NaF radiotracer was then injected into the flow loop. After a 5 minute circulation time to achieve a homogeneous mixture, 10 minutes of imaging was initiated. After the imaging acquisition was completed, the pump was stopped. The in-vitro loop was dismantled and drained. The loop was rinsed with deionized water and a post-PET scan (10 minutes) was then conducted with no solution in the loop and the pump off. This process was repeated for the FDG radiotracer in a second flow loop.

Analysis was completed on the reconstructed images using the ASIPro software. Regions-of-interest were manually drawn over the images in full field of view and the mean voxel values of

the counts were determined. The net activity of each PET radiopharmaceutical in the scan was obtained by summation of activity in consecutive coronal slices. The mean, standard deviation, minimum and maximum of the total radioactivity were computed and summarized for each scan. The pump parameters including power, speed, and estimated flow were collected at 50Hz and statistically analyzed with Minitab 15 (Minitab; State College, PA). Baseline pump parameters were compared to pump parameters during administration of radiotracers and PET scans.

## **RESULTS**

This study showed no real-time operational changes in the HeartWare MVAD pump during administration of both radiopharmaceuticals and PET scanning. Minimal changes in power consumption (W) were observed with close to no change in speed (RPM) and estimated flow (L/min) between baseline and treatment conditions (Table I). There was no statistical difference of pump parameters between baseline and treatment and no difference between FDG and NaF (all p-values  $\geq 0.27$ ). Real-time data parameters collected during the FDG and NaF loop studies can be seen in Figure 3. Controller log files downloaded after studies revealed no alarms or events triggered during pump operation. Battery power consumption and discharge rates were linear with no abnormalities.

Each PET scan resulted in 64 slices with the pump imaging limited to only 30 to 40 of these slices. The regions of interest were drawn over the areas in these slides where the pump resided. Table II provides the total radioactivity during radiotracer circulation and after draining the in-vitro loop for both NaF and FDG. The mean residual radioactivity was less than 1% for both radiotracers after circulation and draining of the in-vitro loop. Imaging of the pump during tracer circulation showed little artifact or scattering. Figure 4 and Figure 5 provide cross-section and 3D composite images taken during circulation of each radiotracer. The images showed clear flow paths for the

inflow, outflow, and volute portions of the pump. Imaging was obscured at the portion of the pump where the impeller was operating inside the motor core as seen in Figure 6.

## **DISCUSSION**

The primary results from this study show no interaction of radiotracers and PET imaging to system operation of the MVAD pump, external controller, and battery components. There are no electrical components housed in the pump, only the stator core and wires contained in the driveline connecting the motor to the controller. The housing of the pump is composed of a titanium alloy and ceramic assembly with the impeller composed of magnetized platinum cobalt (4-5). With no sensitive electrical components in the pump, there is significantly less risk for interference or pump failure. The external controller that connects to the percutaneous driveline from the pump contains the microprocessors that operate the pump, manages power, and stores diagnostic information. This controller is not in the direct path of treatment though may be susceptible to radiation damage. Though if controller components are damaged leading to fault or failure of the controller, it can be replaced with a back-up as the controller is external to the body.

The secondary results of this study were imaging and retention of radiotracers inside the pump. Previous testing completed by the investigators with x-ray and proton radiation therapies on the currently used HVAD pump (HeartWare) device showed scattering and attenuation of imaging and dose delivery (16,17). PET imaging reported in this study show clear imaging of inflow and outflow regions of the pump with obscured imaging in the portion of the pump where the impeller is spinning (Figure 6). It is unknown why imaging was not possible in this area though likely related to the small radial gaps and high velocity of the fluid through the spinning impeller (8,000 to 18,000 RPM). The residual radioactivity after completion of imaging was minimal and expected. It is important the tracers do not have an affinity to the pump so that they can be taken

up by the targeted body tissue to be imaged instead of the pump components. Less than 1% was retained after circulation and due to the short half-life of the tracers, this residual amount will be gone within a short time after treatment.

Application of PET scanning for direct imaging of a ventricular assist device has been limited to detection of VAD related infections (1,13,15). These studies demonstrate increased cell metabolic rate activity in areas that have VAD related infections in the driveline exit site and the outflow cannula extremity. PET may allow for early detection of infection as well as evaluation of response to treatment therapies. Infection is a significant source of adverse events and a major factor limiting the further expansion of the VAD therapies. This nuclear modality may not be exclusive to infections. Potential use could be applied to detection of pump related thrombus inside the pump, inflow cannula, or outflow graft. PET has been utilized to detect and determine the age of deep vein thrombosis (1,18). This application may be useful in the VAD population to determine location (inflow vs outflow), size, and age of thrombus. Further testing will be needed for feasibility of this imaging application.

## **SUMMARY/CONCLUSION**

Ventricular assist device implantation continues to grow as transplantation rates remain constant and the heart failure patient population increases. Therapies and diagnostic evaluations routinely used in hospitals need to be reviewed for use in VAD patients. Potential interactions between the life-sustaining devices and therapies must be carefully considered to decrease the risk for inaccurate diagnostics (imaging), incomplete treatment delivery, or pump failure. PET may have additional utility outside of the current use in detection of infection. In this in-vitro study no interaction was observed between the HeartWare MVAD pump and direct PET imaging with two commonly used radiotracers. Clear imaging of the internal pump components were possible with

minimal retention of radiotracer in the pump components following circulation.

## **REFERENCES:**

1. Dembitsky WP, Tector AJ, Park S, et al. Left ventricular assist device performance with long-term circulatory support: lessons from the REMATCH trial. *Ann Thorac Surg.* 2004 Dec;78(6):2123-2130.
2. Wohlschlaeger J, Schmitz KJ, Schmid C, et al. Reverse remodeling following insertion of left ventricular assist devices (LVAD): a review of the morphological and molecular changes. *Cardiovasc Res.* 2005 Dec;68(3):376-86.
3. Tuzun E, Roberts K, Cohn W, et al. In vivo evaluation of the HeartWare centrifugal ventricular assist device. *Texas Heart Institute Journal.* 2007;34(4):406-411.
4. Slaughter MS, Giridharan GA, Tamez D, et al. Transapical miniaturized ventricular assist device: design and initial testing. *J Thorac Cardiovasc Surg.* 2011 Sep;142(3):668-674.
5. McGee Jr E, Chorpenning K, Brown MC, et al. In vivo evaluation of the HeartWare MVAD. *J Heart Lung Transplant.* 2014 Apr;33(4):366-371.
6. Popov AF, Hosseini MT, Zych B, et al. Clinical experience with HeartWare left ventricular assist device in patients with end stage heart failure. *Ann Thorac Surg.* 2012 Mar;93(3):810-815.
7. Wilson S, Givertz MM, Garrick CS, Stewart C, Mudge GH. Ventricular assist devices: the challenge of outpatient management. *J Am Coll Cardiol.* 2009 Oct;54(18):1647-1659.

8. Slaughter MS, Sobieskii MA, Tamez D, et al. HeartWare miniature axial-flow ventricular assist device. Design and initial feasibility test. *Texas Heart Inst J.* 2009;36(1):12-16.
9. Deuse T, & Reichenspurner H. Do not touch the sternum-thoracotomy incisions for HVAD implantation. *ASAIO J.* 2014 Mar-Apr;60(2):234-236.
10. Sileshi B, Haglund NA, Davis ME, et al. In-hospital outcomes of a minimally invasive off-pump left thoracotomy approach using a centrifugal continuous-flow left ventricular assist device. *J Heart Lung Transplant.* 2015 Jan;34(1):107-112.
11. Tai YF, Piccini P. Applications of positron emission tomography (PET) in neurology. *J Neurol Neurosurg Psychiatry.* 2004 May;75(5):669-776.
12. Duhaylonsod FG, Lowe VJ, Patz EF, et al. Detection of primary and recurrent lung cancer by means of F-18 fluorodeoxyglucose positron emission tomography (FDG PET). *J Thoracic Cardiovasc Surgery,* 1995 Jul;110(1):130-140.
13. Costo S, Hourna E, Massetti M, et al. Impact of F-18 FDG PET-CT for the diagnosis and management of infection in JARVIK 2000 Device. *Clin Nucl Med.* 2011 Dec;36(12):e188-191.
14. Tlili G, Picard F, Pinaquy JB, et al. The usefulness of FDG PET/CT imaging in suspicion of LVAD infection. *J Nucl Cardiol.* 2014 Aug;21(4):845-848.
15. Kim J, Feller ED, Chen W, Dilsizian V. FDG PET/CT imaging for LVAD associated infections. *JACC Cardiovasc Imaging.* 2014 Aug;7(8):839-842.

16. Gossman MS, Graham JD, Tamez D, et al. Evaluation of a ventricular assist device: stability under x-rays and therapeutic beam attenuation. *ASAIO J.* 2012 May-Jun;58(3):1-5.
  
17. Gossman MS, Graham JD, Das IJ, et al. Evaluation of a ventricular assist device system : stability in a proton beam therapy. *ASAIO J.* 2012 Nov-Dec;58(6):597-600.
  
18. Rondina MT, Lam UT, Pendleton RC, et al. F-FDG PET in the evaluation of acuity of deep vein thrombosis. *Clin Nucl Med.* 2012 Dec;37(12):1139-1145.

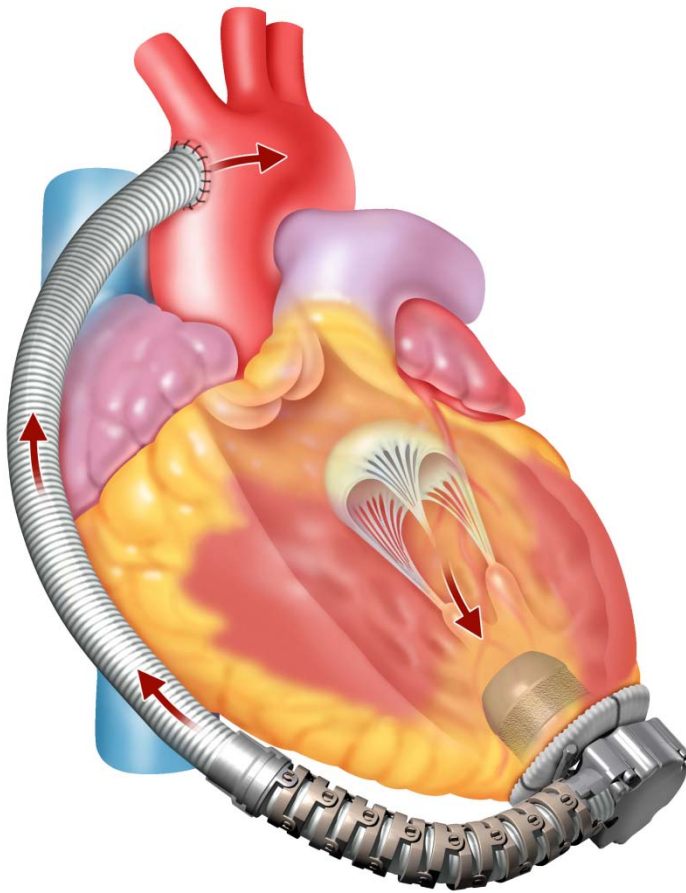


Figure 1. MVAD surgically attached to the heart

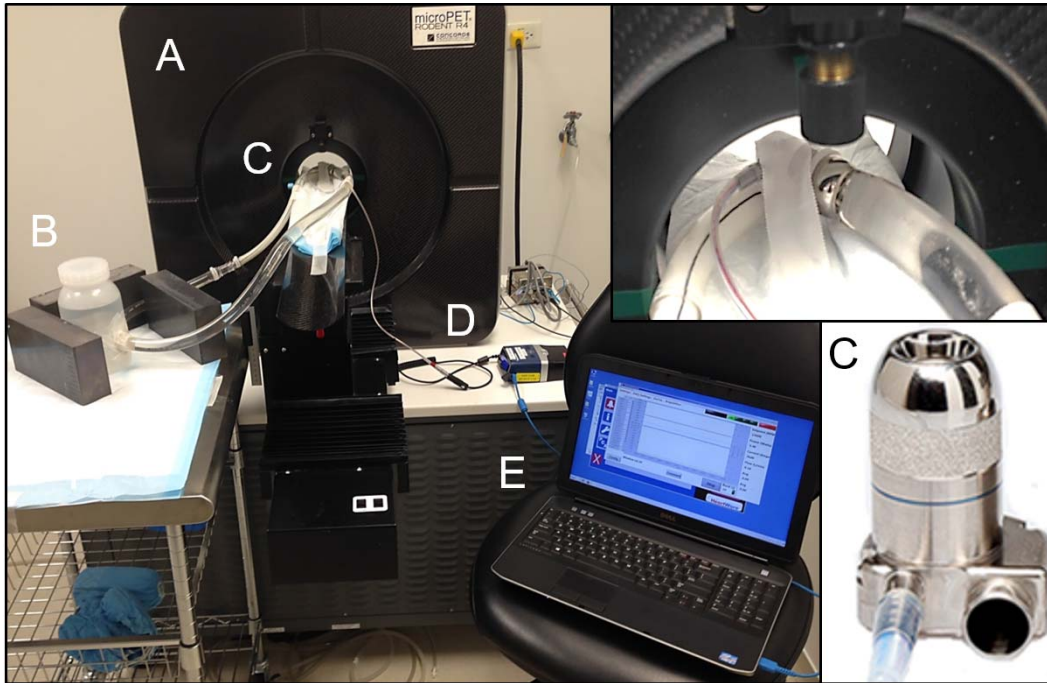


Figure 2. Experimental setup. A) Siemens MicroPET-R4 scanner; B) 1.2 L In-vitro flow loop with lead bricks shielding loop reservoir; C) MVAD pump; D) PAL system controller connected to MVAD pump through driveline; E) Custom data acquisition system, PAL-DAS, used to capture pump operational parameters

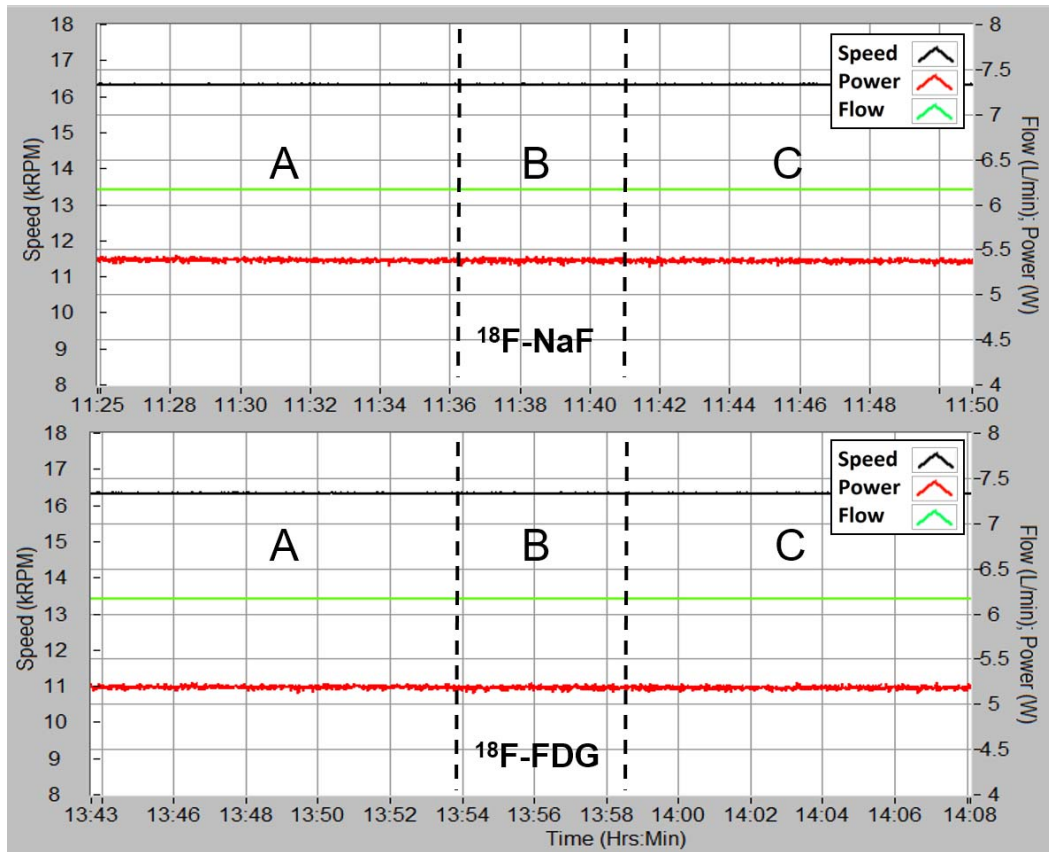


Figure 3. Real-time pump parameters including speed, power, and flow with NaF (Top) and FDG (Bottom) radiotracers. Regions: A – Baseline pump operation; B – Introduction and circulation of radiotracers; C – PET imaging.

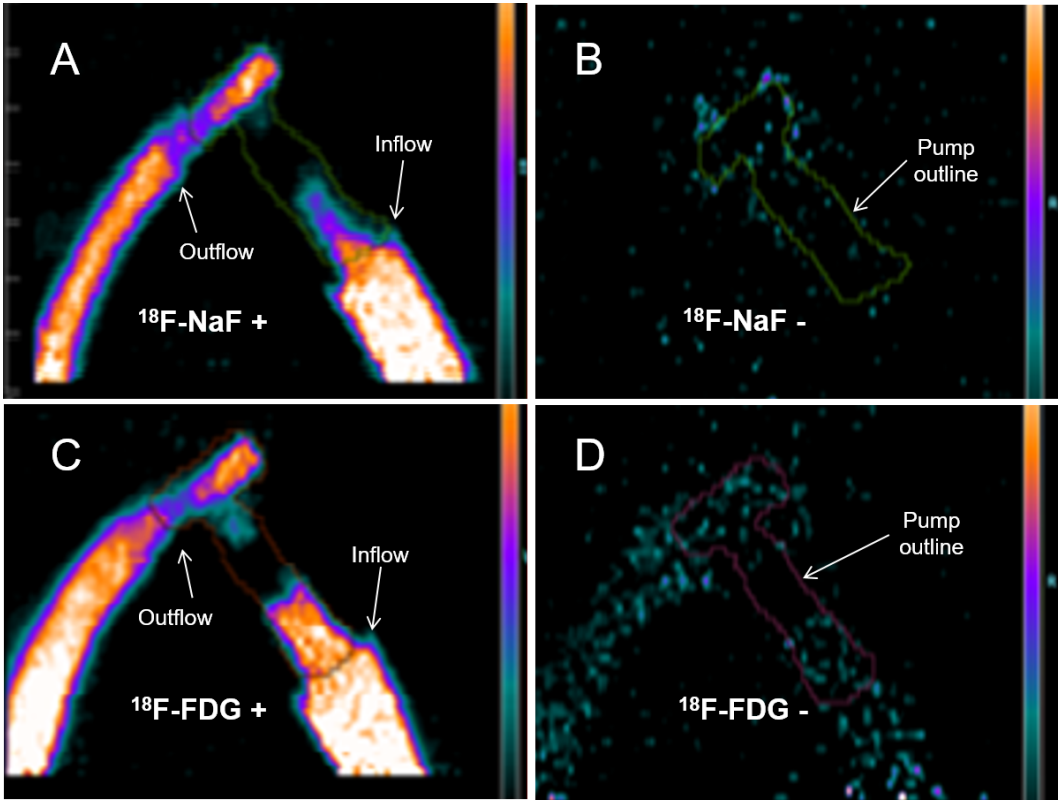


Figure 4. Cross sectional PET imaging of MVAD Pump during circulation of the radiotracers NaF (A) and FDG (C). Images were taken after draining in-vitro loops to find residual radiation for NaF (B) and FDG (D).

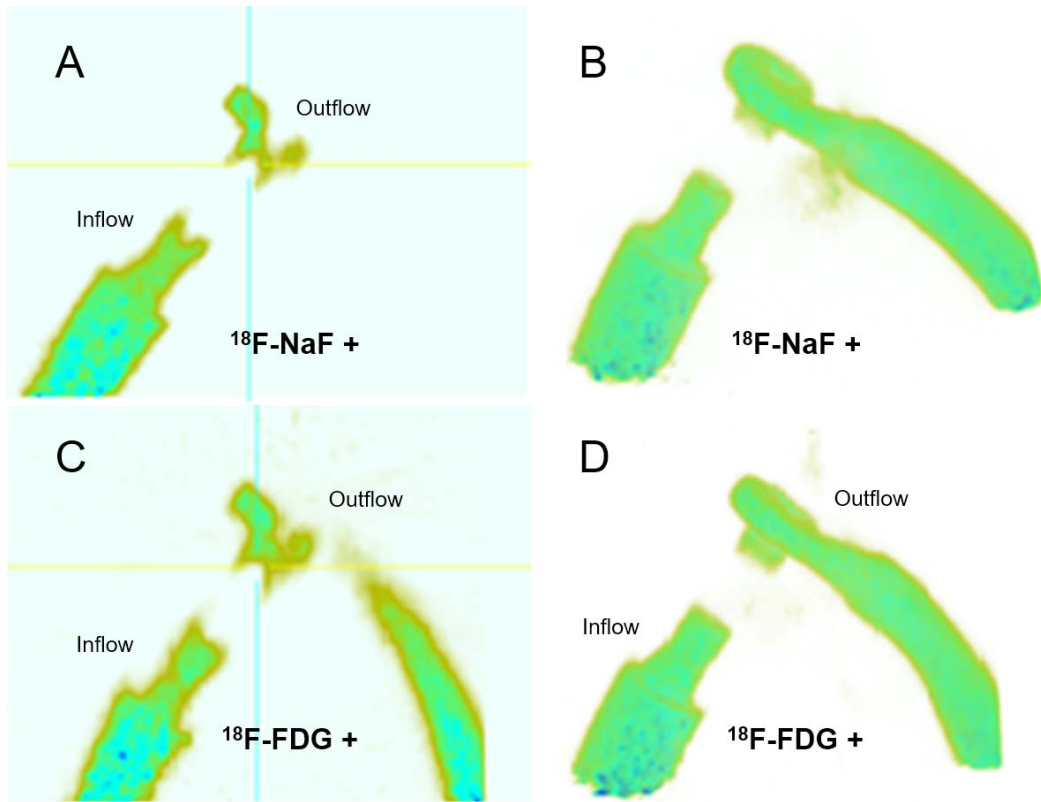


Figure 5. Cross sectional PET imaging of MVAD Pump during circulation of the radiotracers NaF (A) and FDG (C). 3D reconstruction during circulation of the radiotracers NaF (B) and FDG (D)

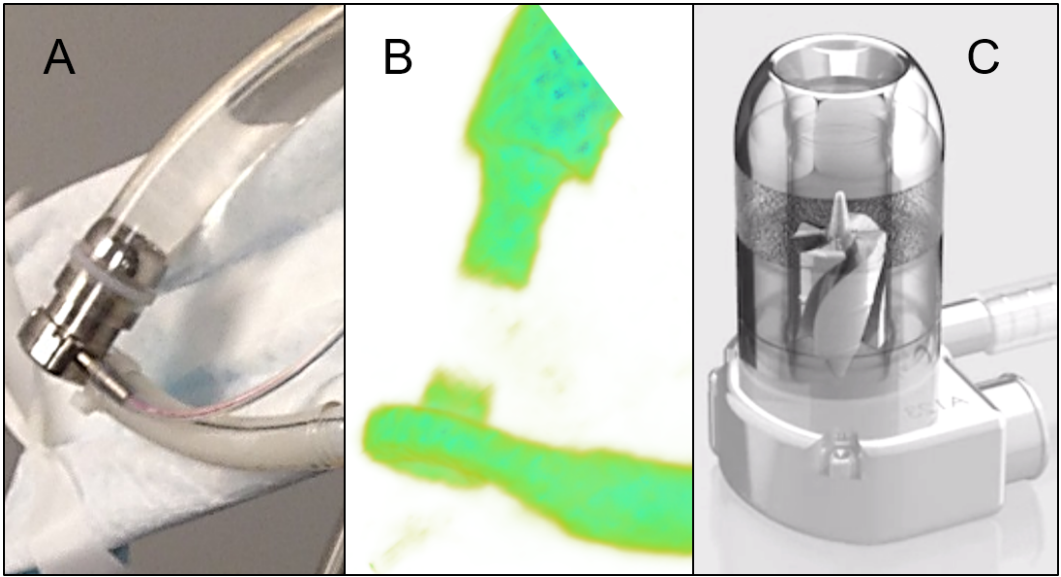


Figure 6. A) MVAD Pump with outflow graft connected to in-vitro flow loop. B) 3D PET image of circulating radiotracer. Imaging was obscured in the region of the pump where the impeller is spinning at 14,000 RPM. C) Drawing of MVAD Pump showing location of suspended rotating impeller.

Radiotracer	Baseline pump parameters			Treatment pump parameters		
	Power (W)	Flow (L/min)	Speed (RPM)	Power (W)	Flow (L/min)	Speed (RPM)
<b>NaF</b>	5.39 ± 0.02	6.16 ± 0.00	14999 ± 3	5.37 ± 0.02	6.16 ± 0.00	14999 ± 3
<b>FDG</b>	5.19 ± 0.02	6.16 ± 0.00	14999 ± 3	5.19 ± 0.02	6.16 ± 0.00	14999 ± 3

Table I. Pump Parameters Baseline and Treatment for NaF and FDG

<b>Radiotracer</b>	<b>Total radioactivity</b>		<b>% retention</b>
	<b>(nCi/cc)</b>		
	Treatment	Posttreatment	
<b>NaF</b>	587.1 ± 772.9 (3,184.9)	1.8 ± 5.1 (101)	0.31%
<b>FDG</b>	627.6 ± 802.3 (3,122.2)	3.8 ± 7.9 (93.1)	0.61%

Mean ± Standard Deviation (Maximum)

Table II. Total Radioactivity at Treatment and Post-Treatment